

In vitro antibacterial activity of electrolytic silver nanoparticle against *Staphylococcus aureus*

 Suparno Suparno^{1*}, Deby Grace¹, Khafid Nur Aziz¹, Dwandaru Wipsar Sunu Brams¹, Eka Sentia Ayu Lestari¹

¹Fakultas MIPA, Universitas Negeri Yogyakarta, Jl Colombo no 1, Depok, Sleman, Yogyakarta 55281, Indonesia; suparno_mipa@uny.ac.id (S.S.).

Abstract: This paper reports a research project aimed at uncovering the antibacterial activity of electrolytic silver nanoparticles (ESN) against *Staphylococcus aureus* (*S. aureus*) with a focus on efficacy and power to prevent resistance. ESN is produced by electrolysis method. The silver content in the solution was characterized with a UV-visible spectrophotometer and the particle size was determined using dynamic light scattering (DLS). The antibacterial activity of silver nanoparticles was assessed using the Kirby-Bauer method. UV visible spectrometer measurements show an absorption wavelength peak of 414nm indicating that the solution contains silver atoms. The DLS measurement results show that the average ESN size is 93nm, the polydispersity index is 0.1579, and the size distribution is a single modal distribution graph showing small broadening. Raw data showed that chloramphenicol produced significantly higher efficacy than ESN. However, they are measured in different units (chloramphenicol in % and ESN in ppm). Analysis using a calibration curve shows that at the same concentration ESN 5% produces almost 85 times the efficacy compared to chloramphenicol 5%. Data also showed that *S. aureus* developed resistance to chloramphenicol after 42 hours. In contrast, it did not show resistance to ESN at all concentrations until the last observation at 48 hours indicating the power of ESN to prevent *S. aureus* resistance. These two findings show that ESN has extraordinary potential as a raw material for future antibacterial agents.

Keywords: Antibacterial agent, Chloramphenicol, Disk diffusion method, Silver nanoparticle, *Staphylococcus aureus*.

1. Introduction

Rapid growth of new strains [1], more vicious bacteria [2], and the development of bacteria resistance [3] to many different medicines have been challenging for decades. Many researches have been conducted by countless people around the world to develop powerful antimicrobial medicine, however the results are still behind the expectation [4]. Not to mention huge investment spent by pharmaceutical industries along with sophisticated technologies and skillful human assets to find such medicine. Many types of bacteria seem easier to find their way to adapt with different environment, human immune system, and many different new drugs [5]. Finding new and powerful antimicrobial medicine is becoming more challenging [6].

Staphylococcus aureus (*S. aureus*) bacteria belong to a type of bacteria being able to adapt with many different chemical antibacterial medicines [3]. Several types of *S. aureus* are known to be multi resistant to various drugs [7]. These Gram-positive bacteria has relatively thick cell wall and form biofilm as part of their survival against antibody and antimicrobial drug [8]. Many efforts have been done to combat these bacteria, unfortunately these bacteria are still stand strong and new strains of *S. aureus* are born [9].

Since many species of bacteria develop resistance to chemical antibacterial agents, many researchers have turned to develop physical antibacterial agents. Platinum, gold, and silver nanoparticles have been proven to have antibacterial activity with different efficacy [10], [11]. The choice of developing these

such nanoparticles is not only based on the noble metal [12] but also on the small size of nanoparticles [13]. The minute size of nanoparticles enables them to interact with more bacteria compared to the bulk particle and subsequently kill more bacteria. Since the cost of material of the first two types of nanoparticles is relatively expensive, more researchers are focusing on the development of low-cost silver nanoparticles [12]. Many published researches showed that silver nanoparticles have antibacterial activities with different efficacy to different types of bacteria [14], [15].

In this study, we report silver nanoparticle synthesis using electrolysis technique [16]. The formation of silver nanoparticles was monitored once every 10 minute and results were reported here. The presence of silver nanoparticles was assessed using UV visible spectrophotometer and the size of nanoparticles was determined using particle size analyzer employing dynamic light scattering (DLS) [17]. The antibacterial tests of silver nanoparticles at three different concentrations were conducted using Kirby-Bauer disk diffusion method [18] and the results were juxtaposed to that of chloramphenicol 5%. Statistical analyses were done to compare the efficacy between these three concentrations of silver nanoparticles and to compare the efficacy of silver nanoparticles and chloramphenicol. More detailed analysis was done using a calibration curve to predict efficacy of 5% silver nanoparticles and compare with 5% chloramphenicol of 5. In addition, the power to prevent *S. aureus* resistance development was compared between ESN and chloramphenicol [19].

2. Materials and Method

2.1. Silver Nanoparticle Formation

Figure 1 shows an electrolysis instrument for silver nanoparticles formation. It employs a pair of silver slabs with 3mm in thickness, 4mm in width, and 15mm in length as positive and negative electrode. This silver slabs were prepared by heating and molding 400 grams of silver (AgBr) granules. A direct current power supply was used to drive both electrodes at 24 Volts. These two electrodes were set in parallel arrangement one facing another at 10 mm separation hanging on home-made black rubber cap of a brown bottle. Most electrodes were immersed in 400 ml volume of water.

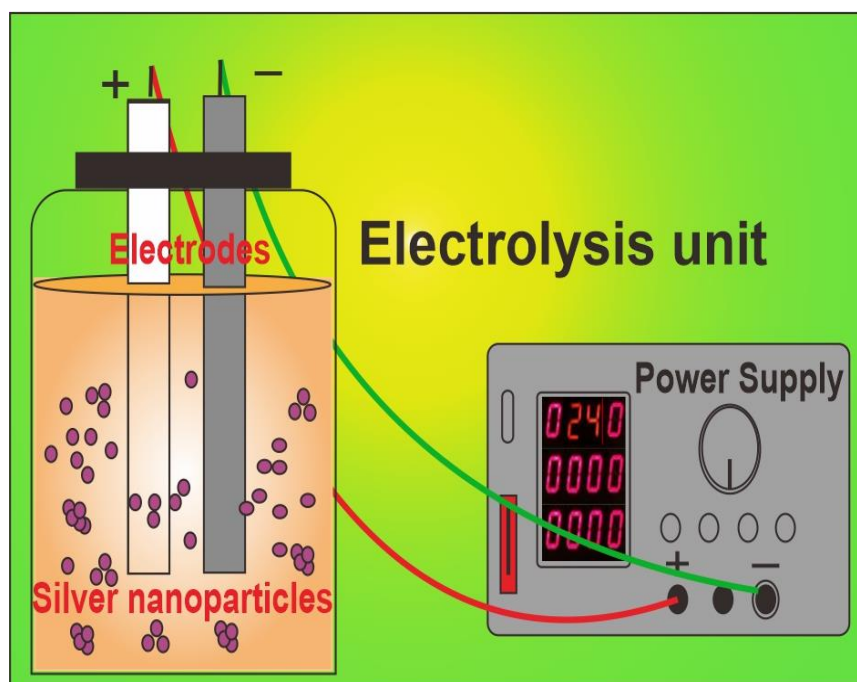
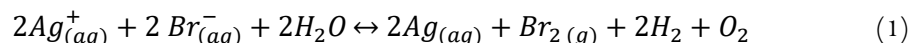


Figure 1.
Electrolysis unit for generating silver nanoparticles.

Silver bromide is sparingly soluble in water [20] with solubility of 1.3×10^{-7} g AgBr/L. The silver atom (Ag) formation ionization process is given by



resulting in two silver atoms and one bromide gas molecule. It is believed that silver nanoparticles are formed by the aggregation of these silver atoms. The low and slow solubility of AgBr in water apparently becomes a blessing in disguise in the production of relatively small size silver nanoparticles. Slow and low solubility of AgBr in water leading to relatively slow silver nanoparticle formation. Therefore, we believe this technique is suitable for smaller size particle formation such as silver dots.

Here are what to do to produce silver nanoparticles aggregation using electrolysis technique. Firstly, fill the brown bottle with 400 ml of distilled water. Secondly, place the rubber lid along with the two silver bromide electrodes on the bottle. Then connect the two cables (red and green) to 24 Volts DC power supply. Either connection will do since both silver electrodes are identical, so that they are interchangeable. Set the voltage at 24 Volts and the current at 2 Amperes. Check all the connections as in Figure 1 before final step placing the switch on. Measure the concentration of silver nanoparticle in part per million (ppm) using TDS-meter and write the data down once in 10 minutes for a period of 70 minutes.

2.2. Silver Nanoparticle in Solution

The presence of silver nanoparticle in solution is determined using UV visible spectrophotometer [21]. In practice, a sample of around 4 ml silver nanoparticle solution is placed in a cuvette. Another cuvette containing the same volume of solvent was also prepared for the measurement of the solvent absorption. The sample and solvent were scanned together from (200 – 800) nm and the difference between the two gives the absorption of the silver nanoparticles. After simple analysis the results were displayed as absorbance as a function of absorption wavelength. The presence of silver in the detected solution is represented by the absorption peak wavelength. The silver nanoparticle absorption peak wavelength usually falls in between 400 nm – 450 nm [22].

2.3. Particle Size Determination

Nanoparticle is defined as a particle of (1-100) nm in size [23]. Since the sample is in form of solution and the silver nanoparticles were formed by aggregation, DLS was chosen to characterize their size instead of SEM or TEM. The DLS technique was chosen since the sample for this technique is maintained in real condition (solution) during measurement, so that the measured size represents its real size. It does not need any treatment such as evaporation, coating, or vacuuming that changes the size from the real size.

The measurement of silver nanoparticles diameter in this research was done using particle size analyzer (PSA) employing dynamic light scattering technique. The technique was quite straight forward by firstly injected 5 microliter silver nanoparticle solution into the small cylindrical sample cell. Then adjust some constants and variables such as identity of the sample, wavelength of light, viscosity of the solution, refractive index, and room temperature need to be input. Set the sample time at 60 seconds and repetitions at 5 times and run.

The detector receives scattered light intensity fluctuations and analyzed the size of spectral broadening to yield the particle size. Unlike other DLS technique interfering scattered light and incident light to produce heterodyning process, PSA superimposing scattered light and reflected light and send these signals to the detector through a fiber optic. In practice, the measurement of each sample will be complete in 5 minutes and the summary of the result is shown in Figure 4.

2.4. Antibacterial Activity Assessment

The antibacterial activity observation began with nutrient broth (NB) and nutrient agar (NA) preparation. NB powder product of Himedia M002-500 was used in this research. The NB preparation began by dispersing 1.3 g NB powder into a total volume of 100 ml distilled water and mixing the dispersion to ensure the homogeneity of the dispersion. It was then sterilized using autoclave at 15 psi

at 121° C for 15 minutes. Only after NB being sterilized, *S. aureus* was inoculated into. This research used *S. aureus* culture ATCC 6538 with designated strain FDA 209 which was released on 29 December 2020. The same bacteria used in our previous research [24]. The liquid NB containing *S. aureus* in a conical flask was incubated in incubating shaker for 24 hours to allow the growth of bacteria. Finally, the NB was stored in refrigerator at 5°C in a culture bottle before being used.

The solid medium NA was prepared firstly by dispersing 2.8 g Himedia M001-500 powder to a total volume of 100 ml distilled water. Secondly, this dispersion was mixed thoroughly by using a glass mixing rod. The dispersion was then sterilized using autoclave at 15 psi at 121° C for 15 minutes. The hot dispersion was cooled down for 10 minutes before being poured into 5 petri dishes under laminar flow cabinet and let them to solidify at room temperature. All solid NA in petri dishes were then dried for 24 hours in incubator and finally stored in refrigerator at 5° C before being used.

The clear zone diameter measurements were done in a petri dish containing NA which was spread with *S. aureus* taken from NB bottle. Using Drigalski spatula the *S. aureus* was spread evenly on the surface of NA. Three impregnated disks containing 10 ppm, 30 pm, 50 ppm silver nanoparticle solutions, one containing chloramphenicol 5% and one containing water were placed in the same petri dish separately. The three-silver nanoparticle impregnated disks were given code names of A, B, and C, chloramphenicol 5% as positive control [25] and water as negative control were given code name of D and E respectively. Lastly, the clear area around these 5 disks were measured in horizontal, vertical, and diagonal ways using a digital caliper. The measurements were conducted once in every 3 hours over a period of 48 hours.

3. Results and Discussions

3.1. Silver Nanoparticle Formation Profile

Table 1 shows ESN concentrations produced in time produced by electrolysis. ESN concentration was measured once in every 10 minutes for a period of 70 minutes and recorded in part per million (ppm) unit.

Table 1.
Concentration of silver nanoparticle in time.

Time (minute)	10	20	30	40	50	60	70
Concentration (ppm)	2	17	34	44	46	48	50

The data shows rapid aggregation of silver nanoparticles in the first 40 minutes resulting in 44 ppm concentration of silver nanoparticles, followed by very slow formation during the last 30 minutes. Figure 2 shows ESN formation through aggregation process. Figure 2a shows silver atoms production during the first few minutes. Figure 2b shows the presence of silver atoms aggregation. Figure 2c indicates the formation of ESN aggregates. During the last 30 minutes it was only 6 ppm addition silver nanoparticle produced. The slow production of ESN aggregate after 40 minutes was attributed to thin and dark film formation on cathode. This film and dark film slowed down reduction at the cathode and oxidation at the anode so that the production of silver atom decreases drastically after 40 minutes. The process should be stopped at 40 minutes for efficiency. If more concentration is needed, then it should be done through evaporation of the one produced during 40 minutes.

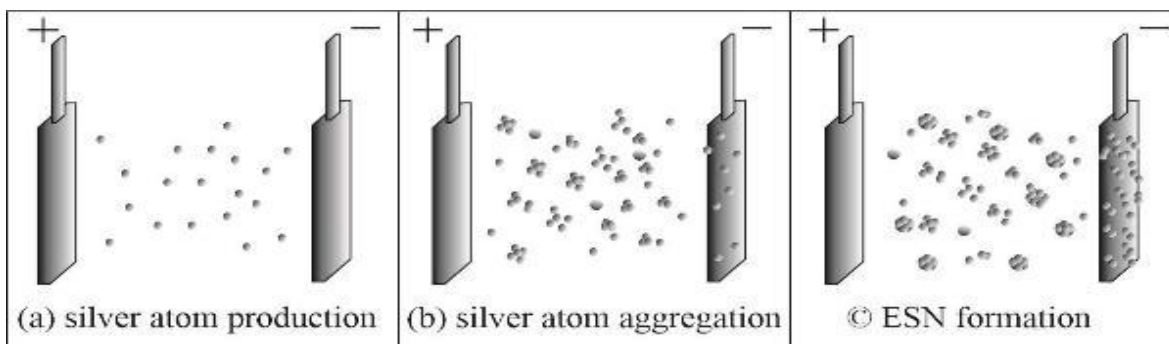


Figure 2.
Electrolytic silver nanoparticle formation.

The concentrations of sample were prepared at 50 ppm, 30 ppm, and 10 ppm, each in 100 ml volume. All these samples were prepared from the 50ppm stock produced by electrolysis process. The dilutions were done from 30 ppm and 10 ppm sample concentrations through Equation (2)

$$C_1 V_1 = C_2 V_2 \quad (2)$$

In this equation C_1 is stock concentration (50 ppm), V_1 is stock volume required for dilution, C_2 denotes target concentration, and V_2 is target volume. Therefore, to prepare 100 ml of 30 ppm sample, requires stock volume V_1 as much as 60 ml. A 40 ml distilled water was then added to the 60 ml of 50 ppm to make up 100 ml of 30 ppm sample. The same way goes to the 100 ml of 10 ppm sample.

3.2. Silver Content of the Solution

Figure 3 shows the absorption peak wavelength of silver nanoparticle solution prepared by electrolysis technique. It was found the silver nanoparticle absorption peak wavelength was 414 nm. It is acceptable number since silver nanoparticle absorption peak wavelength usually falls in between 400 nm – 450 nm [26]. Hashemi S and Givianrad M found silver nanoparticle absorption peak at 413nm and 414 nm [27] Another research group showed silver nanoparticle absorption peak at 410 – 437 nm [28]. They attributed the difference in absorption peak wavelength or red shifted absorption peak wavelengths due to the existence of different chromophores and auxochromes such as carbonyl, carboxyl, and hydroxyl in the solution.

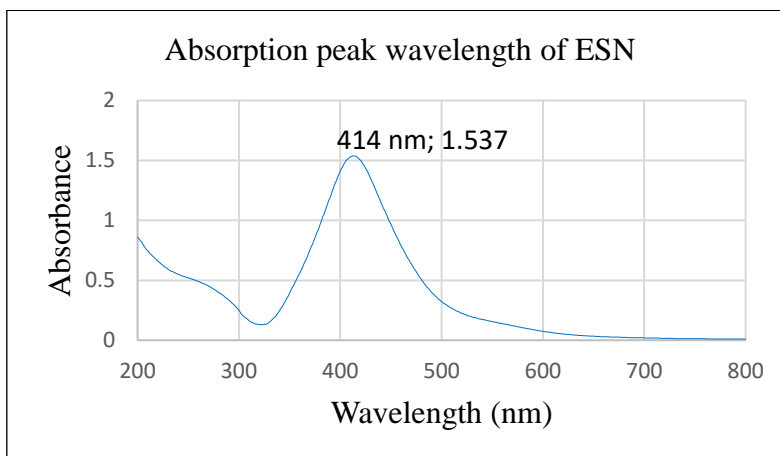


Figure 3.
Absorption peak wavelength of silver nanoparticle.

The absorbance at the peak was recorded as 1.537. This is relatively high absorbance related to the relatively high concentration of silver nanoparticle in the solutions, since the relationship of absorbance and the concentration of the solution is given by Beer-Lambert law stated as $A = \epsilon bc$ [29]. In this

equation, A denotes the absorbance, ϵ represents the molar absorption coefficient, b stands for optical pathlength, and c is the concentration.

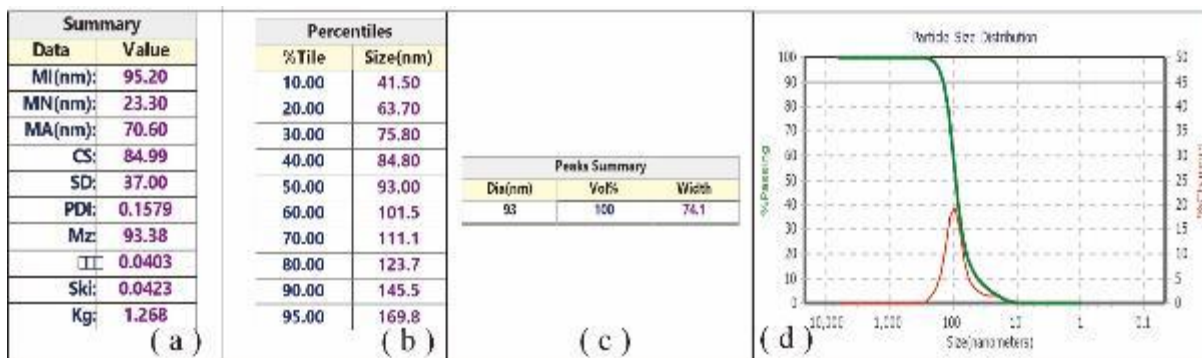


Figure 4.

Polydispersity index, diameter, and size distribution of silver nanoparticle solution.

3.3. Silver Nanoparticle Size

Figure 4 shows the polydispersity index (PDI), the average diameter, and ESN size distribution. The PDI value of 0.1579 in Figure 4(a) shows relatively low value showing good quality of the solution meaning that the sample is relatively homogeneous [30]. This is supported by the size distribution graph (red graph) in Figure 4(d) showing a bell-like single modal distribution graph with relatively small broadening [31]. Small broadening of the graph represents homogeneity of the solution and the single modal distribution graph shows that size of particle is dominated around the size of the single peak. The average size of particles was measured to be 93 nm presented in Figure 4 (c). This value corresponds to the D50 size distribution (Figure 4b) where 50% of the sizes are less than this value (93 nm) and 50% are above it.

DLS was chosen to characterize ESN size instead of SEM or TEM, since it measures the size of particles in real condition as colloidal particles in the dispersion. Therefore, it gives real particle size in real dispersion. It does not require evaporation of the sample solution, since evaporation causes the particles to shrink. Additionally, the nanoparticle aggregation may be de-agglomerated during evaporation [31] to become smaller size particles. It does not require coating, since coating causes the size to increase. The measurement was not done in vacuum. All measurements are conducted in real sample condition. Therefore, the results would represent the real size, do not need correction for shrinking due to evaporation or breaking apart due to aggregation and increasing size due to coating.

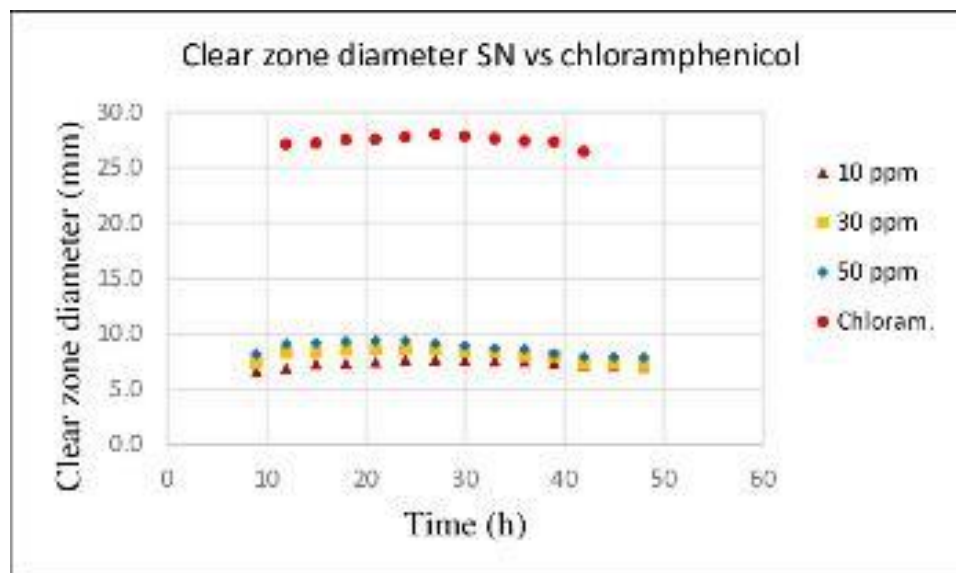


Figure 5.
Clear zone diameters of ESN and chloramphenicol at the stationary stage.

3.4. Silver Nanoparticle Efficacy

The efficacy of antibacterial agent is represented by its clear zone diameter [32]. The clear zone diameter changes all the time during observation following the dynamic interaction between bacteria and antibacterial agent. It was during stationary stage the clear zone diameter relatively stable since at this stage the number of bacterial deaths equals to the number bacteria created naturally. Therefore, the comparison of efficacy between different bacteria is best done at stationary stage [33]. Figure 5 shows the clear zone diameters of ESN at different concentrations and chloramphenicol at the stationary stage. This figure shows the clear zone diameter of chloramphenicol 5% is much higher than ESN (10 ppm, 30 ppm, and 50 ppm). It is also supported by the P values of t-Test analyses shown in Table 2 comparing chloramphenicol and all concentrations of ESN which are all smaller than 0.05, so that all the null hypotheses are rejected. This means that chloramphenicol produces significantly larger clear zone diameters than all ESN concentrations. These results were not a surprised one, since the concentrations of ESN were still very low. The ESN concentration of 50 ppm equals 0.005% ESN, which is still much lower than 5% chloramphenicol.

Table 2.
P values of comparison between chloramphenicol and ESN.

Chlo. 5%	ESN 50 ppm	ESN 30 ppm	ESN 10 ppm	P value
-	v	v	-	0.008508
-	v	-	v	1.58×10^{-7}
-	-	v	v	0.000154
v	v	-	-	6.8×10^{-29}
v	-	v	-	1.55×10^{-28}
v	-	-	v	3.16×10^{-34}

Table 2 shows comparative statistical analysis of ESN 50/30 ppm; 50/10 ppm, and 30/10 ppm which results in P values of 0.008508, 1.58×10^{-7} , and 0.000154, respectively which are all lower than 0.05. Therefore, H_0 hypotheses of these three comparisons are rejected. Therefore, ESN 50 ppm produces a clear zone diameter that significantly larger than 30 ppm and 10 ppm and ESN 30 ppm produces significantly larger clear zone diameter than 10 ppm. These results confirm that ESN produces larger clear zone diameters with increasing concentration. Since ESN clear zone diameter increases with

the increase of concentration, a calibration curve may be made to predict clear zone diameter for relatively high ESN concentration. The calibration curve is basically a graph of clear zone diameter as a function of ESN concentration. The average of clear zone diameter of 10 ppm ESN is 7.4 mm, 30 ppm ESN is 8.1, and 50 ppm ESN is 8.7 mm. The calibration curve drawn based on these data is presented in Figure 6. Using linear regression equation of the calibration curve which is $Y=0.0344X + 7.0521$ the clear zone diameter of 27.4 mm produced by chloramphenicol 5% can be generated by ESN concentration of only 591.5 ppm which is equal to 0.05915 %. This means that efficacy of 0.05915% ESN equals 5% chloramphenicol. Further calculation shows that 5% ESN concentration would produce clear zone diameter of 2318 mm which is 84.6 times larger than that of 5% chloramphenicol. This finding shows the superiority of ESN to chloramphenicol suggesting a promising candidate for future antibacterial agent.

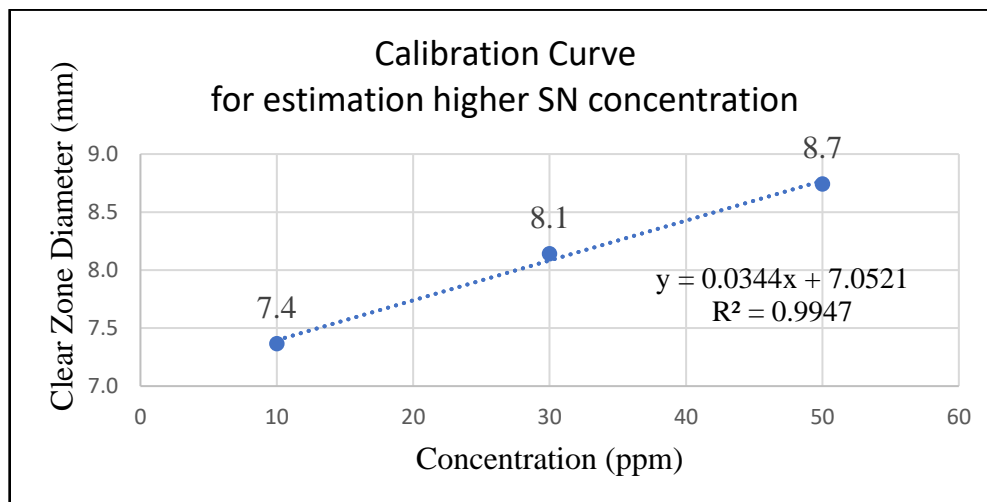


Figure 6.
ESN concentration estimation producing efficacy equivalent to chloramphenicol 5%.

3.5. Resistance Development of *S. Aureus*

Figure 5 also shows that the stationary stage of chloramphenicol dropped off after 42 hours. This means that after 2 hours *S. aureus* develop resistance to chloramphenicol [34]. On the contrary, *S. aureus* does not show resistance to ESN at all concentrations till the end of the observation at 48 hours. These data show that ESN at all concentrations pose more power to prevent the resistance development of *S. aureus* [35]. This result may be explained as follows. Chloramphenicol is bacteriostatic, so that it does not kill *S. aureus*. Instead, it targets ribosome inhibiting *S. aureus* growth [36]. On the contrary, ESN can be both bacteriostatic and bactericides [37]. ESN inhibits bacteria growth by disrupting DNA replication [38]. At the same time, upon contact with *S. aureus* ESN increase *S. aureus* membranes permeability causing the flow of electrolyte to increase (in and out of membrane) leading to the destruction of internal organs which left *S. aureus* to die [39]. This finding reassures that ESN does not only have very strong efficacy, but also strong power to prevent *S. aureus* resistance development.

4. Conclusion

In summary, silver nanoparticles have been successfully produced by electrolysis technique with most efficient production during the first 40 minutes. The UV visible spectrophotometry characterization shows that the ESN absorption peak wavelength is 437 nm and by means of DLS the nanoparticle diameter was found to be 93 nm with polydispersity index of 0.1579 showing relatively low heterogeneity of the sample. Antibacterial activity shows that the efficacy of ESN against *S. aureus* increases with the increase of concentration. By using a calibration curve at the same concentration of 5% ESN would have efficacy nearly 85 times compared to that of chloramphenicol. Furthermore, ESN

has more power to prevent *S. aureus* resistance development than chloramphenicol. These two findings strongly suggest that ESN poses powerful potential as raw material for future antimicrobial medicine.

Author contribution:

S.S. contribute to conceptualization, methodology, analysis, writing manuscript. D.G.: sample preparation, data curation, draft writing. K.N.A.: methodology, investigation. D.W.S.B.: supervision, data analysis. E.S.A.L.: sample preparation, data curation.

Copyright:

© 2024 by the authors. This article is an open access article distributed under the terms and conditions of the Creative Commons Attribution (CC BY) license (<https://creativecommons.org/licenses/by/4.0/>).

References

- [1] R. V. Filimon *et al.*, 'New Malolactic Bacteria Strains Isolated from Wine Microbiota: Characterization and Technological Properties', *Fermentation*, vol. 8, no. 1, 2022, doi: 10.3390/fermentation8010031.
- [2] P. Erichson, 'World Health Organization Food safety', 2019.
- [3] C. K. Ezech, C. N. Eze, M. E. U. Dibua, and S. C. Emencheta, 'A meta-analysis on the prevalence of resistance of Staphylococcus aureus to different antibiotics in Nigeria', 2023. doi: 10.1186/s13756-023-01243-x.
- [4] A. Ebrahimezhad, S.-M. Taghizadeh, S. Taghizadeh, and Y. Ghasemi, 'Chemical and Biological Approaches for the Synthesis of Silver Nanoparticles; A Mini-Review', *Trends in Pharmaceutical Science*, vol. 3, no. 2, 2017.
- [5] A. Sanchini, 'Recent Developments in Phenotypic and Molecular Diagnostic Methods for Antimicrobial Resistance Detection in Staphylococcus aureus: A Narrative Review', 2022. doi: 10.3390/diagnostics12010208.
- [6] K. Lewis, 'At the Crossroads of Bioenergetics and Antibiotic Discovery', 2020. doi: 10.1134/S0006297920120019.
- [7] H. A. Zaher *et al.*, 'Molecular Basis of Methicillin and Vancomycin Resistance in Staphylococcus aureus from Cattle, Sheep Carcasses and Slaughterhouse Workers', *Antibiotics*, vol. 12, no. 2, 2023, doi: 10.3390/antibiotics12020205.
- [8] G. Shaghayegh *et al.*, 'S. aureus biofilm metabolic activity correlates positively with patients' eosinophil frequencies and disease severity in chronic rhinosinusitis', *Microbes Infect*, vol. 25, no. 8, 2023, doi: 10.1016/j.micinf.2023.105213.
- [9] P. Nikolic and P. Mudgil, 'The Cell Wall, Cell Membrane and Virulence Factors of Staphylococcus aureus and Their Role in Antibiotic Resistance', 2023. doi: 10.3390/microorganisms11020259.
- [10] B. Ranpariya *et al.*, 'Antimicrobial Synergy of Silver-Platinum Nanohybrids with Antibiotics', *Front Microbiol*, vol. 11, 2021, doi: 10.3389/fmicb.2020.610968.
- [11] M. Paesa *et al.*, 'Elucidating the mechanisms of action of antibiotic-like ionic gold and biogenic gold nanoparticles against bacteria', *J Colloid Interface Sci*, vol. 633, 2023, doi: 10.1016/j.jcis.2022.11.138.
- [12] L. Ye *et al.*, 'Noble metal-based nanomaterials as antibacterial agents', 2022. doi: 10.1016/j.jallcom.2022.164091.
- [13] X. Yang, W. Ye, Y. Qi, Y. Ying, and Z. Xia, 'Overcoming Multidrug Resistance in Bacteria Through Antibiotics Delivery in Surface-Engineered Nano-Cargos: Recent Developments for Future Nano-Antibiotics', 2021. doi: 10.3389/fbioe.2021.696514.
- [14] H. Salama and M. Shaaban, 'Biological activity of synthesized silver nanoparticles on S. aureus and P. aeruginosa', *Delta Journal of Science*, vol. 46, no. 1, 2023, doi: 10.21608/djs.2023.195872.1080.
- [15] S. K. I. Palupi and S. Suparno, 'Ionic Silver Nanoparticles (Ag+) Sebagai Bahan Antibiotik Alternatif Untuk Salmonella Typhymurium', *INDONESIAN JOURNAL OF APPLIED PHYSICS*, vol. 10, no. 01, 2020, doi: 10.13057/ijap.v10i01.34407.
- [16] C. W. Lai, 'Facile formation of colloidal silver nanoparticles using electrolysis technique and their antimicrobial activity', *Micro Nano Lett*, vol. 13, no. 3, 2018, doi: 10.1049/mnl.2017.0805.
- [17] Z. Jia, J. Li, L. Gao, D. Yang, and A. Kanaev, 'Dynamic Light Scattering: A Powerful Tool for In Situ Nanoparticle Sizing', 2023. doi: 10.3390/colloids7010015.
- [18] H. Yao, J. Liu, X. Jiang, F. Chen, X. Lu, and J. Zhang, 'Analysis of the clinical effect of combined drug susceptibility to guide medication for carbapenem-resistant klebsiella pneumoniae patients based on the Kirby-Bauer disk diffusion method', *Infect Drug Resist*, vol. 14, 2021, doi: 10.2147/IDR.S282386.
- [19] A. A. Joshi and R. H. Patil, 'Metal nanoparticles as inhibitors of enzymes and toxins of multidrug-resistant Staphylococcus aureus', 2023. doi: 10.1016/j.imj.2023.11.006.
- [20] K. Wonner, S. Murke, S. R. Alfarano, P. Hosseini, M. Havenith, and K. Tschulik, 'Operando electrochemical SERS monitors nanoparticle reactions by capping agent fingerprints', *Nano Res*, vol. 15, no. 5, 2022, doi: 10.1007/s12274-021-3999-2.
- [21] I. I. Latumakulita and S. Suparno, 'Characterization of Silver Nanoparticle Electrolysis Method with UV-Vis Spectrometer, Atomic Absorption Spectrophotometer, and Particle Size Analyzer', *Kasuari: Physics Education Journal (KPEJ)*, vol. 5, no. 1, 2022, doi: 10.37891/kpej.v5i1.178.
- [22] R. K. Meena, R. Meena, D. K. Arya, S. Jadoun, R. Hada, and R. Kumari, 'Synthesis of Silver Nanoparticles by Phyllanthus emblica Plant Extract and Their Antibacterial Activity', *Material Science Research India*, vol. 17, no. 2, 2020, doi: 10.13005/msri/170206.

- [23] I. Ijaz, E. Gilani, A. Nazir, and A. Bukhari, 'Detail review on chemical, physical and green synthesis, classification, characterizations and applications of nanoparticles', 2020. doi: 10.1080/17518253.2020.1802517.
- [24] S. Suparno, E. S. Ayu Lestari, and D. Grace, 'Antibacterial activity of Bajakah Kalalawit phenolic against *Staphylococcus aureus* and possible use of phenolic nanoparticles', *Sci Rep*, vol. 14, no. 1, p. 19734, Aug. 2024, doi: 10.1038/s41598-024-70799-4.
- [25] W. Chartarrayawadee *et al.*, 'Green synthesis and stabilization of silver nanoparticles using *Lysimachia foenum-graecum* Hance extract and their antibacterial activity', *Green Processing and Synthesis*, vol. 9, no. 1, 2020, doi: 10.1515/gps-2020-0012.
- [26] A. Najafi, M. Khoeni, G. Khalaj, and A. Sahebgharan, 'Synthesis of silver nanoparticles from electronic scrap by chemical reduction', *Mater Res Express*, vol. 8, no. 12, 2021, doi: 10.1088/2053-1591/ac406d.
- [27] S. Hashemi and M. H. Givianrad, 'Biosynthesis and characterization of silver nanoparticles by using brown marine seaweed *Nizimuddiniazanardinii*', *Indian Journal of Geo-Marine Sciences*, vol. 47, no. 12, 2018.
- [28] M. T. Haseeb *et al.*, 'Linseed hydrogel-mediated green synthesis of silver nanoparticles for antimicrobial and wound-dressing applications', *Int J Nanomedicine*, vol. 12, 2017, doi: 10.2147/IJN.S133971.
- [29] G. Casasanta, F. Falcini, and R. Garra, 'Beer–Lambert law in photochemistry: A new approach', *J Photochem Photobiol A Chem*, vol. 432, 2022, doi: 10.1016/j.jphotochem.2022.114086.
- [30] C. Carbone, C. Caddeo, M. A. Grimaudo, D. E. Manno, A. Serra, and T. Musumeci, 'Ferulic acid-nlc with lavender essential oil: A possible strategy for wound-healing?', *Nanomaterials*, vol. 10, no. 5, 2020, doi: 10.3390/nano10050898.
- [31] P. Ding and A. W. Pacek, 'De-agglomeration of silica nanoparticles in the presence of surfactants', *J Dispers Sci Technol*, vol. 29, no. 4, 2008, doi: 10.1080/01932690701729302.
- [32] C. M. A. L. A. Edon, P. D. Pakan, and C. O. Lada, 'Comparative Test of The Antibacterial Efficacy of Commercial Toothpastes Based on Betel Leaf, Siwak Combination, or Aloe Vera Materials Against *Staphylococcus aureus*', *Cendana Medical Journal (CMJ)*, vol. 11, no. 1, 2023, doi: 10.35508/cmj.v11i1.10496.
- [33] A. V. Ustyuzhanin, G. N. Chistyakova, I. I. Remizova, and A. Makhanyok, 'Genetic determinants of antibiotic resistance in enterobacteria isolated during microbiological monitoring in the perinatal center', *Epidemiologiya i Vaktsinoprofilaktika*, vol. 22, no. 4, 2023, doi: 10.31631/2073-3046-2023-22-4-49-55.
- [34] G. Nemati, A. Romanó, F. Wahl, T. Berger, L. V. Rojo, and H. U. Graber, 'Bovine *Staphylococcus aureus*: a European study of contagiousness and antimicrobial resistance', *Front Vet Sci*, vol. 10, 2023, doi: 10.3389/fvets.2023.1154550.
- [35] F. R. P. Dewi, V. Lim, A. Rosyidah, Fatimah, S. P. A. Wahyuningsih, and U. Zubaidah, 'Characterization of silver nanoparticles (AgNPs) synthesized from *Piper ornatum* leaf extract and its activity against food borne pathogen *Staphylococcus aureus*', *Biodiversitas*, vol. 24, no. 3, 2023, doi: 10.13057/biodiv/d240348.
- [36] J. Yang, J. T. Barra, D. K. Fung, and J. D. Wang, 'Bacillus subtilis produces (p)ppGpp in response to the bacteriostatic antibiotic chloramphenicol to prevent its potential bactericidal effect', *mLife*, vol. 1, no. 2, 2022, doi: 10.1002/mlf2.12031.
- [37] C. Chapa González, L. I. González García, L. G. Burciaga Jurado, and A. Carrillo Castillo, 'Bactericidal activity of silver nanoparticles in drug-resistant bacteria', 2023. doi: 10.1007/s42770-023-00991-7.
- [38] P. R. More, S. Pandit, A. De Filippis, G. Franci, I. Mijakovic, and M. Galdiero, 'Silver Nanoparticles: Bactericidal and Mechanistic Approach against Drug Resistant Pathogens', 2023. doi: 10.3390/microorganisms11020369.
- [39] N. Tripathi and M. K. Goshisht, 'Recent Advances and Mechanistic Insights into Antibacterial Activity, Antibiofilm Activity, and Cytotoxicity of Silver Nanoparticles', 2022. doi: 10.1021/acsabm.2c00014.